Ruthenium– and cobalt–based artificial metalloenzymes for photocatalytic water oxidation in artificial photosynthesis

Polanco Rivas, E.A.

Chapter 1

Introduction

1.Introduction

1.1 Grasping fossil fuels: not a luxury anymore

For half a century, mankind has lived under the premise that fossil fuels are not only the main source of energy but also that it is endless. However, within the years the continuous use and extraction of oil has led to a shortage of oil reserves. In addition, the pollution generated by the burning of this oil has generated an urgent need to develop new and more sustainable energy sources. Around the world, researchers are combining efforts to build systems that can stop our dependency to fossil fuels and save our planet from a possible catastrophic fate. Among all candidates, sun and wind have appeared as suitable replacement for fossil energy resources. Devices capable to drive the generation of power using these sustainable resources are being extensively studied as a major goal towards a more sustainable development of humans on Earth.

1.2 Artificial photosynthesis

One of the oldest and most studied processes performed by nature is photosynthesis. This process takes place in the thylakoid membrane in photosynthetic bacteria in green plants, where a complicated arrangement of proteins manages the light reactions, couple to dark reactions, to convert solar energy into chemical energy (Figure 1.1). The process starts by light–harvesting complexes (LHCs), which absorb solar energy and transfer it to the reaction centre of Photosystem II (**PSII**).[1,2] Here, excitation of pigments of **PSII**, the chlorophyll dimer P680, induces charge separation, thus initiating the water splitting reaction and one of the most uphill processes in nature, called water oxidation. This reaction is promoted by a subunit of PSII called the oxygen evolving center (OEC in Figure 1.1) that contains a Mn_4Ca–oxide cluster, where O_2, 4 H^+ and 4 electrons are produced. Upon making dioxygen and presence of light, one of the side reactions of the system is its own degradation. However, it is also capable of regenerating itself as part of a dynamic cycle called PSII repair cycle.[3] The electrons produced by this first water

oxidation reaction are transported to the second reaction centre of the thylakoid membrane called Photosystem I (**PSI**) *via* electron shuttle molecules called plastoquinones (PQ), cytochrome b6f and plastocyanin (PC). Once at PSI, the electrons reduce the excited chlorophyll pigment $P700^{+}$, formed simultaneously by light irradiation of this reaction center by electron transfer to ferredoxin (Fd), which later activates ferredoxin NADP reductase (FNR) and initiates the production of NADPH, the reduced version of $NADP^{+}$. In parallel, the gradient of protons across the membrane generated by the OEC and via cytochrome b6f is used to synthetize ATP *via* a catalytic molecular machine called ATPsynthase (or ATPase). Finally, a dark catalytic reaction called the Calvin cycle takes place, which converts CO_2 into carbohydrates using the electrons stored in NADPH and ATP.[4,5]

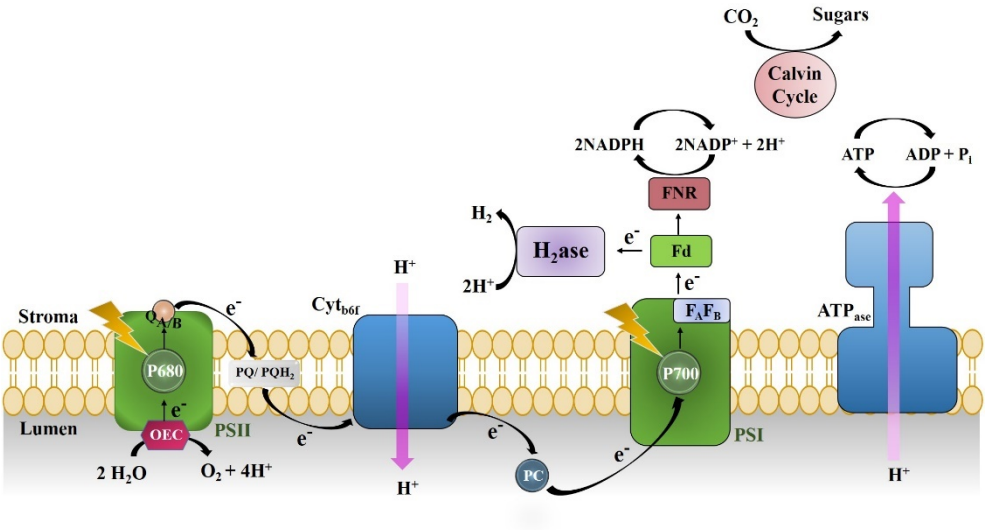

Figure 1.1. Schematic representation of the enzymatic arrangement in the photosynthetic thylakoid membrane.

The idea to replicate the function of the natural photosynthetic system in green plants by building an artificial system capable of transforming sunlight into chemical energy, has become the holy grail of many researchers around the world. These

efforts have allowed the development of several systems, either homogeneous or supramolecular, that promote water splitting into H_2 and O_2. Dihydrogen, in fact, is often considered as one of the most promising alternative energy carriers, not only because it can be burnt directly in a fuel cell to fuel a car or a plane,[6–11] releasing only water as exhaust waste, but also because it can fuel the reduction of many chemicals including CO_2 using existing bulk chemical processes.[12–14]

1.3 Biomimicking the photocatalytic water oxidation reaction

Splitting water involves two half reactions: water oxidation and proton reduction. The former reaction is highly demanding, both thermodynamically and kinetically.[15] The process of extracting four electrons from two very stable water molecules requires a lot of energy and catalytic intermediates. To be able to oxidize water quickly, nature has come up with a manganese catalyst that reduces the energy barrier towards the highest reactive catalytic intermediates of the reaction.[16,17] For biomimicking the natural photocatalytic water oxidation reaction, a minimum of three components are needed: 1) a system capable of harvesting light, called a photosensitizer (PS); 2) a system capable of accepting the electron extracted from water, called an electron acceptor (EA); and 3) a system capable of stabilizing all high-energy intermediates during the reaction, called a catalyst (Cat) (Figure 1.2).

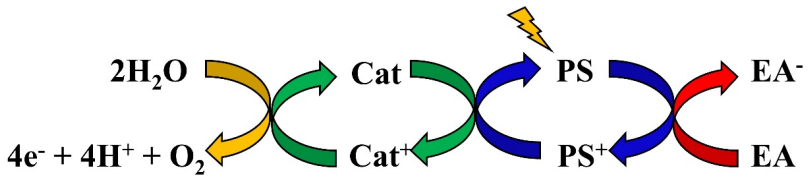

Figure 1.2. General scheme for the minimal system for photocatalytic water oxidation.

By far, $[Ru(bpy)_3]^{2+}$ is the molecule that has the most widely been used as photosensitizer to trigger photochemical reactions.[18–22] For the second component of a photocatalytic system, hence the sacrificial electron acceptor, different compounds have been used, among which sodium persulfate ($Na_2S_2O_8$) and cobalt(III)

pentaamine chloride ($[Co(NH_3)_5Cl]^+$).[23] The third component of the system is the water oxidation catalyst. Small molecules based on different metal centers have been developed to mimic the activity of the biological Mn_4Ca cluster. Most of these complexes are based on noble metals such as ruthenium and iridium.[24] Nevertheless, complexes based on earth-abundant metals such as iron, nickel and cobalt, have gained very much interest as more sustainable candidates. A few example of WOC's are shown in Figure 1.3.[11,23,25–31]

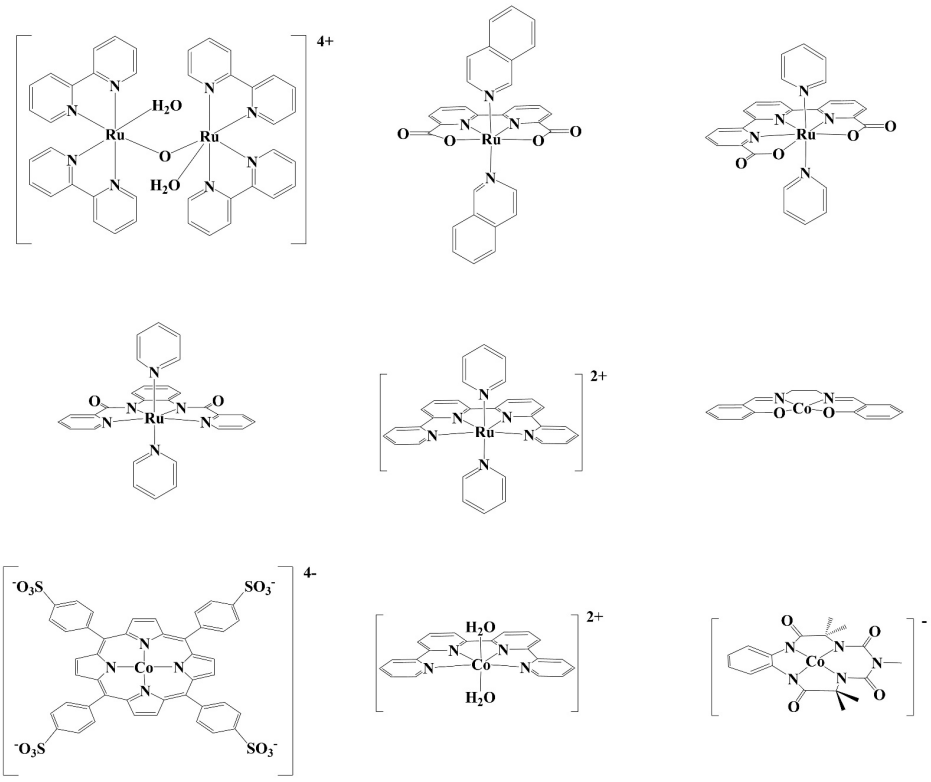

Figure 1.3. Selected examples of ruthenium and cobalt complexes that are catalytically active for water oxidation.

Several limitations in homogeneous photocatalytic systems, such as the low quantum efficiency due to charge recombination,[32–34] the instability of the WOC or photosensitizer under light irradiation,[20] or an overwhelming overpotential of the

catalyst, [35] have stimulated the search for a diversification of methods and strategies towards biomimetic, more efficient, and more stable photocatalytic water oxidation systems.[29,36]

1.4. Artificial metalloenzymes

1.4.1 Proteins, a versatile scaffold

In nature, enzymes represent by excellence the ultimate catalysts, as they allow an incredibly diverse range of biochemical reactions to take place simultaneously in a cell, thus allowing the continuity of life. Efficiency, regioselectivity, stereospecificity, and the ability to catalyse chemical reactions in very mild conditions compared to many industrial, man-made catalysts, are among the attractive features the protein environment can provide for the catalytically active site of enzymes.[37–39] Artificial metalloenzymes (ArMs), which are defined as synthetic conjugates of one or several small-molecule catalysts embedded in a protein environment, have become a promising tool in catalysis.[7,10–16] These artificial systems have provided new solutions to old synthetic problems, allowing to promote reaction such as Diels–Alder,[47] C–H activation,[48] epoxidation,[49] Friedel–Crafts,[50] cyclopropanation,[51] or metathesis,[52] possible in mild conditions and with very good to excellent rates. Using a protein as a scaffold to host an artificial catalyst can offer benefits for tuning the activity and selectivity of this catalyst; in particular, it allows to control the first and the second coordination sphere (Figure 1.4).[46,53–55] The first coordination sphere is often intrinsic to the ligand set installed around a metal center, but it can also change upon binding of the catalyst to the protein backbone *via* coordination of a histidine (imine), cysteine (thiolate), aspartic acid (carboxylate), or methionine (thioether) residue. The second coordination sphere can stabilize a cofactor or facilitate the approach of the substrate, for example *via* hydrogen bonding, π–π stacking, or a hydrophobic interaction. Both, in principle, can lead to an increase (or decrease) of the catalytic activity. Last but not least, proteins are

chiral, enantiomerically pure molecules, which can induce regio- or stereo-selectivity *via* interaction of the reagent or product with the catalytic pocket.[39,50]

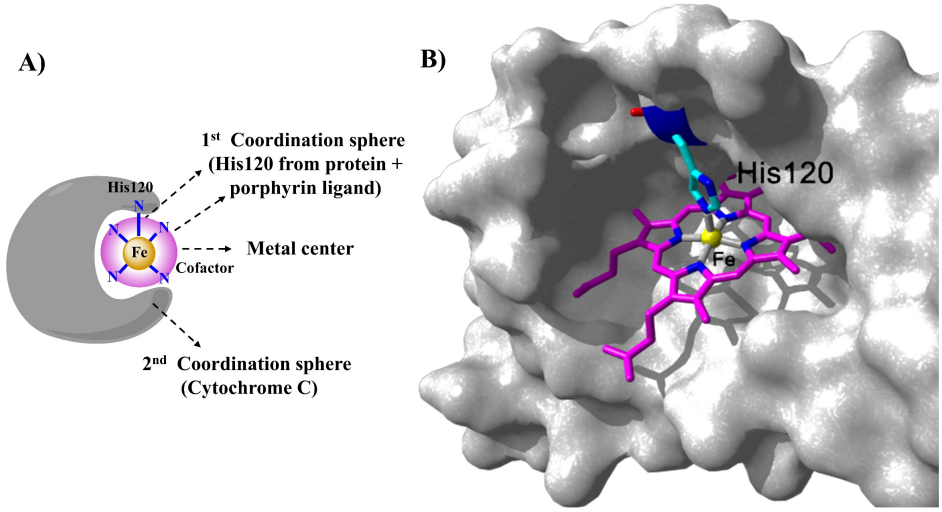

Figure 1.4. (A) Schematic representation of protein scaffold and cofactor coordination environment of Cytochrome C. **(B)** Representation of binding pocket of Cytochrome C (PDB:*1CGO*). The grey colour represents the hydrophobic aminoacids located in the catalytic pocket. The haem group is shown in magenta colour, with Fe(II) center coordinated to the residue His120 in yellow.

When looking at the protein scaffold of ArM's, four strategies to produce artificial metalloenzyme have been investigated: 1) protein re-design, in which the protein scaffold can be modified to enhance the selectivity towards a cofactor or to create new active sites, by introducing mutation in the protein scaffold. Bos *et al*. for example introduced artificial aminoacids in the LmrR protein monomer to create a new active site in the dimer interface which was capable to drive Diels-Alder reaction with 99% enantiomeric excess (ee);[47] 2) supramolecular assembly, where the re-arrangement of proteins units into larger structures is generated by metal-templated assembly. Song *et al.*, for example, produced an artificial β-lactamase assembly using Cytochrome cb562 as building block and Zn^{2+} as metal center to coordinate the protein units;[56] 3) miniaturization, in which a biomimetic version of the protein active site is prepared. With their hydrogen evolution cobalt-

mimochrome VI, for example, Firpo *et al* developed an artificial mini-protein containing a cobalt deuteroporphyrin;[57] 4) and *de novo* design, which is based in the development of a protein from zero. *For example,* Ishida *et al.* developed an artificial ruthenium protein using an unnatural bipyridine-aminoacid in a peptide sequence which coordinated Ru^{2+}.[58]

In all these 4 strategies, a synthetic or man-made compound called an artificial cofactor, $\mathbf{M}^{+}$, is usually used as catalytic center. Few approaches have been proposed to bind these cofactors to a protein scaffold: 1) dative binding, 2) covalent binding, and 3) supramolecular binding (Figure 1.5).[38,59] The dative approach consists in direct coordination of the metal center from the artificial cofactor ($\mathbf{M}^{+}$) to the protein scaffold *via* a coordinating aminoacid residue (Figure 1.5A). This strategy stablishes secondary requirements for the cofactor due to the high selectivity (in terms of size and shape) of the cofactor-binding pocket. In particular, its lipophilicity, aromaticity, planarity, size, and charge, are very important. An example of this approach was presented by Hayashi *et al*. who produced an artificial Myoglobin for C(sp3)-H bond hydroxylation by replacing the natural porphyrin haem cofactor of Myoglobin by a manganese porphycene (Figure 1.6A).[60] Metal exchange, where only the native metal center of the protein is replaced, can also be classified as part of the dative approach (Figure 1.5D). The replacement of the natural metal ion of the enzyme for another one with different chemical properties, usually redirects, and sometimes enhances, the catalytic properties of the enzyme. Okrasa and Kazlauskas, for example, showed a remarkable example of this strategy by replacing the native zinc ion (Zn^{2+}) of Carbonic Anhydrase (CA) by a manganese center (Mn^{2+}).[61] This artificial manganese-carbonic anhydrase metalloenzyme showed peroxidase activity towars *o*-dianisine oxidation comparable with horseradish peroxidase (k_{cat}/K_M = $1.4x10^6$ $M^{-1}s^{-1}$ vs k_{cat}/K_M = $57x10^6$ $M^{-1}s^{-1}$ respectively), in addition to being enantioselective for olefins epoxidation to epoxides.

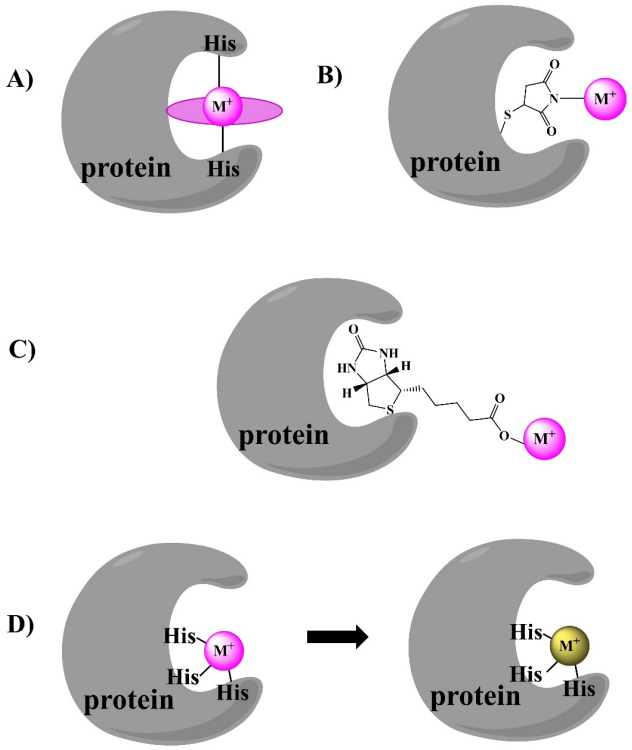

Figure 1.5. Four main strategies for making artificial metalloenzymes. **(A)** the dative strategy; **(B)** the covalent strategy; **(C)** the supramolecular strategy; (**D**) metal exchange. The metal center of the artificial cofactor, $\mathbf{M}^{+}$, is represented in colour (pink or yellow). The pink circle in A) represents an equatorial ligand bound to the metal cofactor $\mathbf{M}^{+}$.

The covalent binding strategy represents a versatile method to attach an artificial cofactor to a protein. In addition to the often higher stability of covalent bonds compared to coordination bonds, further modification on the protein scaffold can be bypassed and only modifications in the artificial cofactor are required, which can enhance the selectivity of the functionalization or the ratio between the protein and the cofactor (Figure 1.5B). In this strategy, the complex must be derivatized prior to protein binding in order to introduce the functional group that will allow covalent coupling to the protein scaffold. For example, Peterson *et al*. showed ruthenium-cytochrome c bioconjugates activated by light irradiation by coupling a photoactive ruthenium complex to the protein *via* maleimide-cysteine bond (Figure 1.6B).[62] In

addition, increasing the selectivity of the binding towards the artificial cofactor can be performed by modification of the residues in the catalytic pocket using mutations. Monnard *et al*. described how mutations on the protein scaffold of an artificial iridium-human carbonic anhydrase enhanced the imines hydrogenation activity.[63] A more synthetically challenging strategy involves the modification of the natural cofactor of the protein to introduce an artificial functional group. This strategy often increases the selectivity of the interaction between the whole artificial cofactor ($\mathbf{M}^+$) and the protein, as recognition of the natural cofactor is always built in the protein backbone. Such strategy was approached by Immoos *et al*. who modified a Haem with a $-(CH_2)_7-$ linker bound to a ruthenium complex to study the electron transfer between the photoactive complex and the myoglobin native iron cofactor (Figure 1.6C).[64] Finally, the supramolecular approach is the most used strategy, because it is synthetically often easier (Figure 1.5C).[48,65] The versatility of this method relies on the multiple supramolecular interaction a metal complex might have with a protein backbone (e.g., hydrogen–bonding, hydrophobic interaction, electrostatics, sterics) and the possibility of the molecule to interact in more than one location. In this strategy, the selectivity of protein binding can be very high, in particular if there is a good fit between the shape of the molecule and that of the binding pocket. A good example of this strategy was described by Ghirlanda *et al*. in which streptavidin hosted an iron-cluster to biomimic the [Fe-Fe] hydrogenase (Figure 1.6D).[66]

The meticulous selection of the proper protein scaffold to develop an artificial metalloenzyme depends mostly on the final application.[67] However, many proteins have demonstrated a tremendous versatility showing different functions by hosting a large variety of cofactors $\mathbf{M}^+$ with different activities. Among those proteins we can highlight Carbonic anhydrase (**CA**), Myoglobin (**Myb**) and Bovine serum albumin (**BSA**), which are some of the selected proteins as candidates for developing the ArMs described in this PhD thesis. In addition, a haem-protein, Cytochrome B5 (**CB5**), will be studied as fourth candidate to develop ArM.

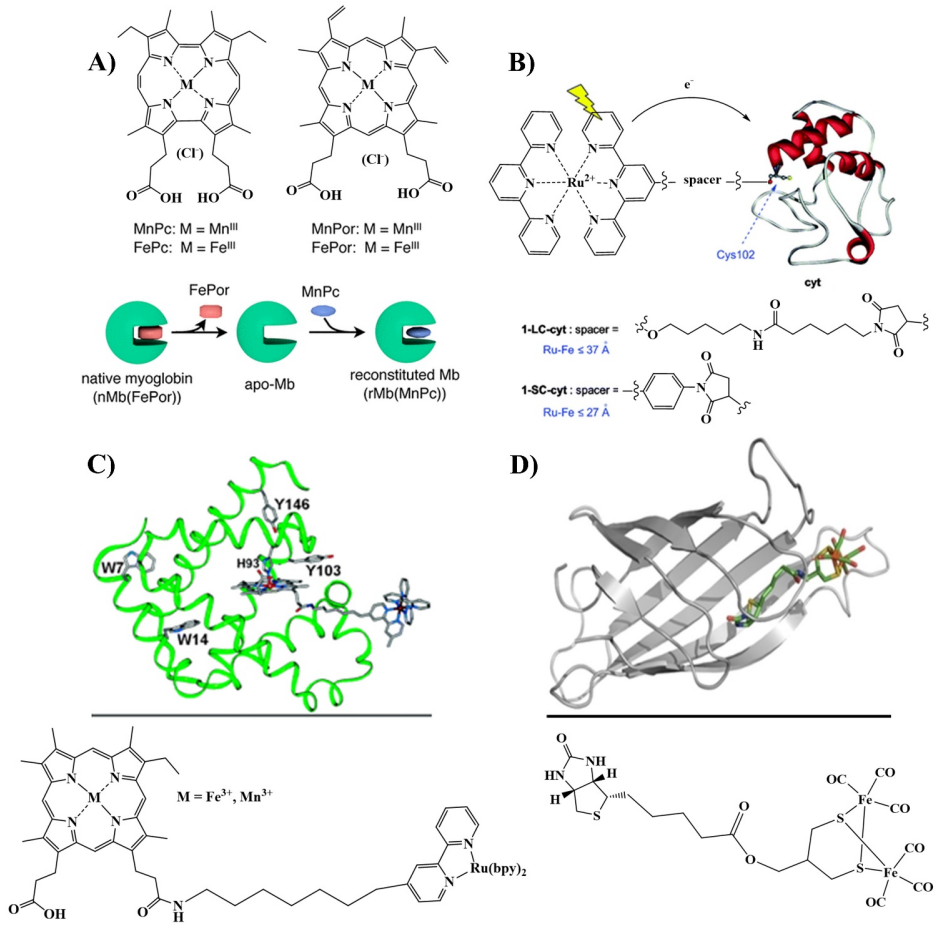

Figure 1.6. Different strategies for making ArM's. **(A)** Artificial Myoglobin for C(sp3)-H bond hydroxylation (*dative strategy*). The replacement of the natural Fe-porphyrin by an Mn-analogue porphyrin facilitated the protein-cofactor interaction. Adapted from reference 58. **(B)** Artificial photoactive Ru(bisterpyridine)-cytochrome c bioconjugates (*covalent bond strategy*). The available Cys102 allows the binding of the Ru(bisterpyridine)-linker complex via maleimide-thiol strategy. Adapted from reference 60. (**C**) Artificial Ru−linker−(haem)-modified myoglobin for electron transfer studies (*covalent bond strategy*). Top: crystal structure of Myb-Ru adduct; bottom: modified Fe-porphyrin-linker-Ru complex. Adapted from reference 62. (**D**) Artificial streptavidin-based [Fe-Fe] hydrogenase (*supramolecular strategy*). Above the Streptavidin protein structure with the biotin-iron complex and below the structure of the biotin-iron-cobalt complex. Adapted from reference 64.

1.4.2 ArM's based on Carbonic anhydrase

Carbonic anhydrase (**CA)** is the first zinc protein discovered in human history; it was originally described by Keilin and Mann as early as 1940. The active site of this protein consists of a Zn^{2+} ion coordinated to four ligands: three histidines that belong to the protein backbone, and one water molecule from the solvent, thus forming a tetrahedral local geometry for the metal center (Figure 1.7A). The water molecule interacts also with a nearby threonine residue (Thr) *via* hydrogen bonding, as a pre–arrangement step of the CO_2 hydration catalytic cycle of **CA**. This ubiquitous enzyme regulates pH by catalysing the reversible hydration of CO_2 and dehydration of HCO_3^- (Figure 1.7B).[68,69]

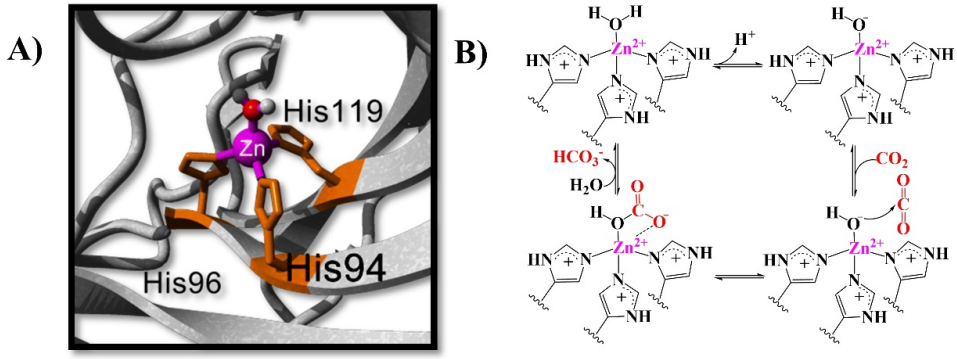

Figure 1.7. (A) Representation of bovine carbonic anhydrase structure (**BCA**) binding pocket (PDB: *2NN7*). **(B)** Protein catalytic cycle for CO_2 hydration.

CA is a monomeric, soluble, and very well-studied protein, characterized by a molecular weight of ~30 kDa. In addition, it is easy to handle and purify, and it is cheap. The active site of this protein has been studied in great details, as well as the substrates that can bind to it with high affinity, thus inhibiting its catalytic function.[68–72] Because it is easy to handle and given its role in many biological processes, **CA** has been used as a model system to study enzymes, and has become a target for biomedical applications. In addition, some studies have shown that **CA** is involved in natural photosynthesis where it controls bicarbonate formation.[73,74] For

these reasons, many compound have been developed to target **CA**, among which aryl sulfonamides that were shown to be **CA** inhibitors with particularly strong interaction with the **CA** binding pocket.[75] **CA** has become a versatile tool for building diverse ArMs with other catalytic activity.[61,63,76] A conjugated system of bovine carbonic anhydrase and 1-palmitoyl-2-oleoyl-sn-glycero-3-phosphoethanolamine-N-(glutaryl) (NGPOPE) liposomes was produced by Maeshima and Yoshimoto, in which the system showed activity towards the production of calcium carbonates particles.[77] Another example of the versatility of CA is reported by Fu *et al*., who showed the production of a biomimetic membrane using **CA** for CO_2 capture in ambient condition operation (room temperature and atmosphere pressure).[78] Overall, this protein is a very promising candidate for developing ArMs.

1.4.3 ArM's based on Cytochrome B5

Cytochromes are proteins in which haem is the natural cofactor. Different types exist (a,b,c or d), depending on how the haem group is bound to the protein scaffold as well as on the axial ligand(s) that is/are bound to the haem group.[79] Cytochrome B5 (**CB5**) is a globular small protein (~12 kDa) which participates in the cellular respiration process. It interacts mainly with cytochrome P450, acting as an electron transport agent in the membrane (Figure 1.8B).[80–82] The haem in this protein is the b type, which coordinates with two histidine residues aligned in axial position, His63 and His39, and does not make any covalent bond with the protein scaffold (Figure 1.8A). The general interest of the ArM community for **CB5** has not been particularly high, but the chemical properties of this protein makes it particularly interesting for applications in redox catalysis.[82–85]

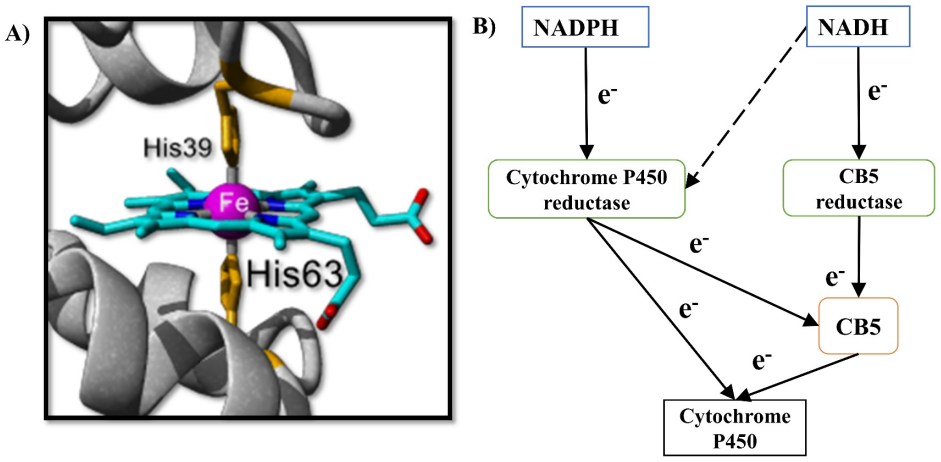

Figure 1.8. (A) Representation of the binding pocket of Cytochrome B5 (PDB:*1CYO*). **(B) CB5** in the electron transport pathways to cytochrome P450 in the endoplasmic reticulum**.** Adapted from reference 81**.** Dotted line represents the alternative pathway of NADH as electron donor**.**

1.4.4 ArM's based on Myoglobin

Myoglobin (**Myb)** is one of the most studied proteins. It has been the subject of an intense scrutiny that has revealed both its structural and catalytic properties. This relatively small protein (~153 aminoacids, 17 kDa) can be found in high amounts in the muscles and was one of the first proteins to be studied by crystallography.[86] The active site of Myb consists in a haem molecule bound to the protein backbone *via* a coordination bond to a single histidine residue (His93, see Figure 1.9A). Being analogous to one fourth of haemoglobin, it plays the role of a final oxygen carrier in muscles. This function is made possible due to the "free" axial position *trans* to the coordinated His93 residue on the iron center, where a coordinated water molecule can easily be displaced by O_2. In addition, a distal histidine can be located (His64) near the binding pocket, at a distance that does not allow for direct coordination of the histidine nitrogen to occur. This distal histidine is vital for the oxy/deoxy myoglobin binding mechanism, stabilizing O_2 binding *via* hydrogen bonding and destabilizing CO binding (Figure 1.9B). Given the remarkable stability of this protein, its application for the development of artificial

metalloenzymes is very appealing. An example of this potential was illustrated by Winter *et al*. who produced a modified Ru-Myoglobin ArM by replacing the natural haem cofactor by a unnatural ruthenium-porphyrin complex; the resulting ArM showed good O_2 sensing properties.[87] Another example of using **Myb** for organic synthesis was proposed by Sreenilayam *et al*., who showed that porphyrin-**Myb** conjugates had an increased activity and selectivity in the cyclopropanation of alkenes *via* carbene transfer.[88] Overall, hundreds of ArM's have been created using **Myb** as a protein scaffold to promote several chemical reactions using diverse strategies, from incorporation of a modified natural haem cofactor to modification of the protein scaffold to anchor an artificial cofactor.[55,60,64,89–93]

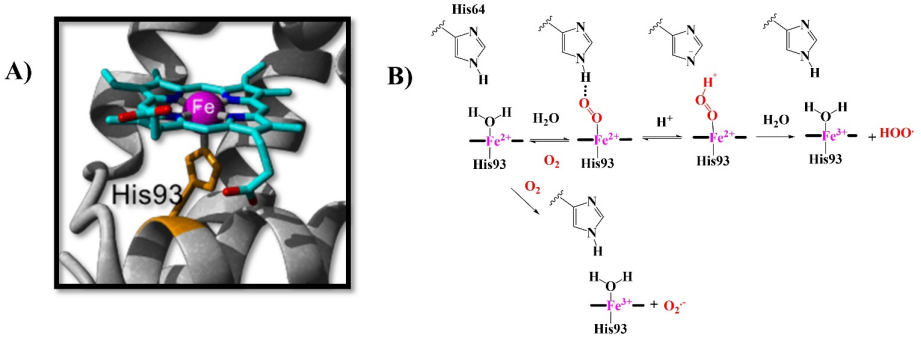

Figure 1.9. Myoglobin (**Myb**). (**A)** Representation of the protein binding pocket. (**B)** Oxy/deoxy myoglobin mechanism (PDB:*5D5R*).

1.4.5 ArM's based on Serum albumin

Serum albumin is the most abundant protein in blood plasma and is present in most vertebrates. It was one of the first proteins to be discovered as well. Its biological function is to carry, deliver, and distribute diverse types of compounds to the body.[94] Bovine serum albumin (**BSA**) is one of the most common albumin to be used in research. It has ~583 aminoacid residues and a molecular weight of ~67 kDa. **BSA** has a characteristically low number of tryptophan residues (Trp134 and Trp212), sixteen crosslinked cysteine residues (hence 8 disulfide bonds) which

stabilize the protein, and one free cysteine, Cys34, that cannot enter into making disulfide bonds (Figure 1.10).

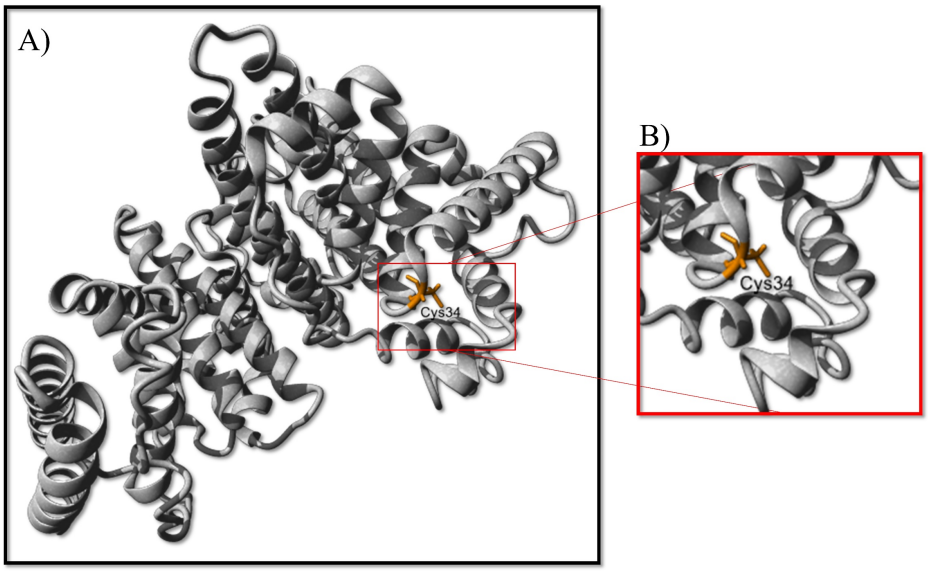

Figure 1.10. Representation of bovine serum albumin (**BSA**). **(A)** Protein secondary fold. **(B)** Free cysteine (Cys34) highlighted in orange in the protein backbone. (PDB:*3V03*)

BSA has three different domains, I, II and II, and each of those domains is composed of two sub–domains. This globular protein is rich in ionic residues which facilitates its solubility even a neutral pH. The binding pocket of **BSA** is hydrophobic but it is known to be able to bind small hydrophobic molecules in other sites as well. One of the characteristic residues of **BSA** is Cys34, which given the selectivity of thiol groups towards functional groups such as maleimides, makes **BSA** attractive synthetically speaking for anchoring synthetic molecules. A recent example reported by Feng *et al*. consisted in a BSA-gallium ArM based on maleimide-thiol strategy allowing the coupling of a ^{68}Galium-labeled tracer for positron emission tomography application (PET).[95] This is one of the many examples where **BSA** and **HSA** have been studied for drug delivery.[94,96–103]

1.5 ArM's for artificial photosynthesis

1.5.1 Artificial metalloenzymes for the H_2 evolution reaction (HER)

In the last decade the catalytic applications of ArM's has expanded in many fields of research, one of which is artificial photosynthesis.[5,104–110] The idea of mimicking nature's multi–enzymatic arrangement in the thylakoid membrane to use water as electron source and sunlight as a sustainable energy to produce H_2 or reduce CO_2 into fuels, is one of the biggest challenges of modern chemistry. ArM's have shown remarkable activity in particular for the production of H_2.[111–113] Call *et al*. developed a protein for hydrogen evolution based on a cobalt-streptavidin conjugate capable to reduce water electro- and photocatalytically, where the protein scaffold not only increased the efficiency up to 14 times (TON and TOF) compared with the free complex, but also reduced the overpotential (100 mV). [114] Sommer *et al*. showed how to incorporate a Co(II) protoporphyrin IX into an *apo*-myoglobin scaffold to give an artificial Co(II)P-**Myb** conjugate which raised four times the H_2 production TON, compared to the free cobalt porphyrin, with a TON of 518 in presence of $[Ru(bpy)_3]^{2+}$ as photosensitizer and sodium ascorbate as electron donor at neutral pH.[55] Another example was presented by Soltau *et al*. who developed an hybrid system using ferredoxin as host for a ruthenium photosensitizer and a cobalt catalyst which drove H_2 production under photocatalytic conditions with a TON of 650. [115] Despite staggering efforts to develop proteins for water reduction and/or hydrogen production, reports addressing the production of artificial metalloenzymes for O_2 evolution are almost non-existent; we discuss the few existing ones in the next paragraph.

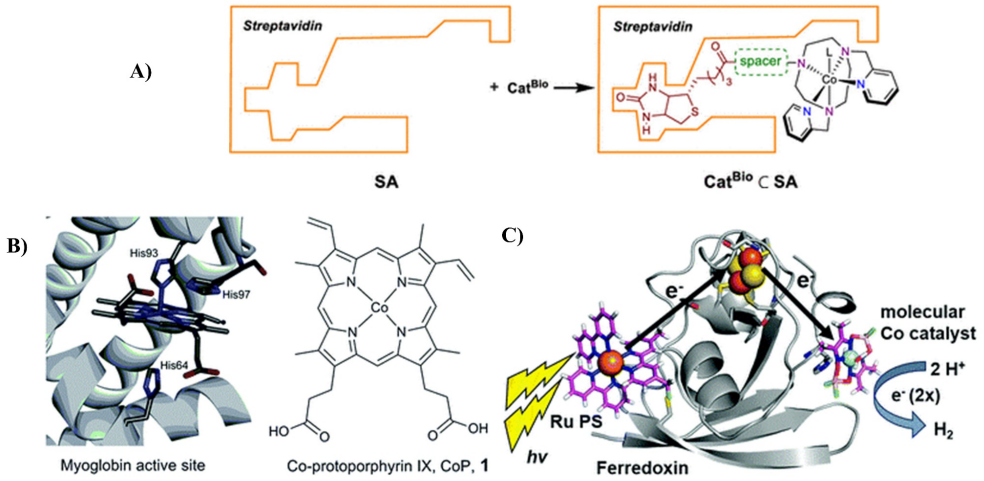

Figure 1.11. (**A**) Scheme for the production of an artificial cobalt metalloenzyme for water reduction using the biotin-streptavidin supramolecular strategy. **SA** refers to the streptavidin scaffold, **Cat^{Bio}** refers to the biotin-spacer-cobalt complex. Taken from reference 109. (**B**) Myoglobin binding site and Co-protoporphyrin IX (CoP, 1) for H_2 production artificial metalloenzyme. Taken from reference 106. (**C**) Artificial ruthenium-ferredoxin-cobalt ArM for H_2 production. Taken from reference 109.

1.5.2 Artificial metalloenzymes for the O_2 evolution reaction (OER)

Essentially, artificial protein-based systems for water oxidation are mostly based on isolated **PSII** proteins fixed into a hybrid system such as a nanostructured electrode (*i.e.*, ITO), which was further integrated into a photoelectrochemical cell.[116,117] Even if this approach is attractive to optimize the conditions for solar cell developments, PSII is a fragile protein and not realistic to consider such systems for solar fuel production. Overall, the idea of using an artificial metalloenzyme for water oxidation has not been considered very seriously, and examples of ArM's for water oxidation are rare. One of the reasons might be the known instability of the Mn_4Ca cluster of **PSII** under light irradiation and the difficulty to reproduce artificially the self–repair mechanism established by natural evolution, which takes place every ~30 min. However, protein models have been prepared that mimic the **PSII** Mn_4Ca WOC. In 2018, Olshansky *et al.*[118] reported an electrochemical study of a metalloprotein for water oxidation containing a cobalt–cubane cofactor bound using

the biotin–streptavidin strategy. This system showed similarities to the Mn_4Ca cluster of **PSII**, notably in the way the tyrosine residues that are involved in the mechanism for the oxygen evolution were influenced by pH changes (Figure 1.12A). This study showed the importance of the protein scaffold for the stabilization of the catalytically active site *via* hydrogen bonding. Another example was published by Kim and Lee,[119] who reported an iridium–modified **CA** protein. In this ArM, the zinc center coordinated to the three histidines of the binding pocket, was replaced by an Ir^{3+} ion (Figure 1.12B). Here, the transmetallation approach redirected the function of the protein to create an ArM capable of performing chemical water oxidation at pH 7 driven by $NaIO_4$ as oxidant, with a TOF of 39.8 min^{-1}. Interestingly, even if the natural cofactor of **CA** is Zn^{2+}, the authors reported that Ir^{3+} showed better affinity for the protein, and that iridium binding did not alter the protein integrity. An additional example of ArM for the OER was introduced by Abdi *et al.*[120] who reported the use of ferritin to host several iron centers (Figure 1.12C). In this strategy, the protein was not modified and only acted as a host that interacted in a dative way with the iron ions. Ferritin promoted the creation of a matrix of iron clusters that showed catalytic activity for electrochemical water oxidation at pH 11 with a TOF of 0.001 s^{-1} at a potential of 1.7 V vs NHE. More recently, Casadevall *et al.*[121] reported an artificial Cytochrome C that bore a Co(II) protoporphyrin IX artificial cofactor. This approach, which was based on a dative anchoring strategy, simply replaced the natural cofactor of the enzyme, Fe(II)–porphyrin IX, by its cobalt(II) analogue (Figure 1.12D). The protein was immobilized in an Sb/SnO_2 anode and it proved to promote O_2 evolution in photoelectrochemical conditions at pH 5 with a TON = 671. To our knowledge, there is no published example of ArM for the OEC reaction in photocatalytic conditions.

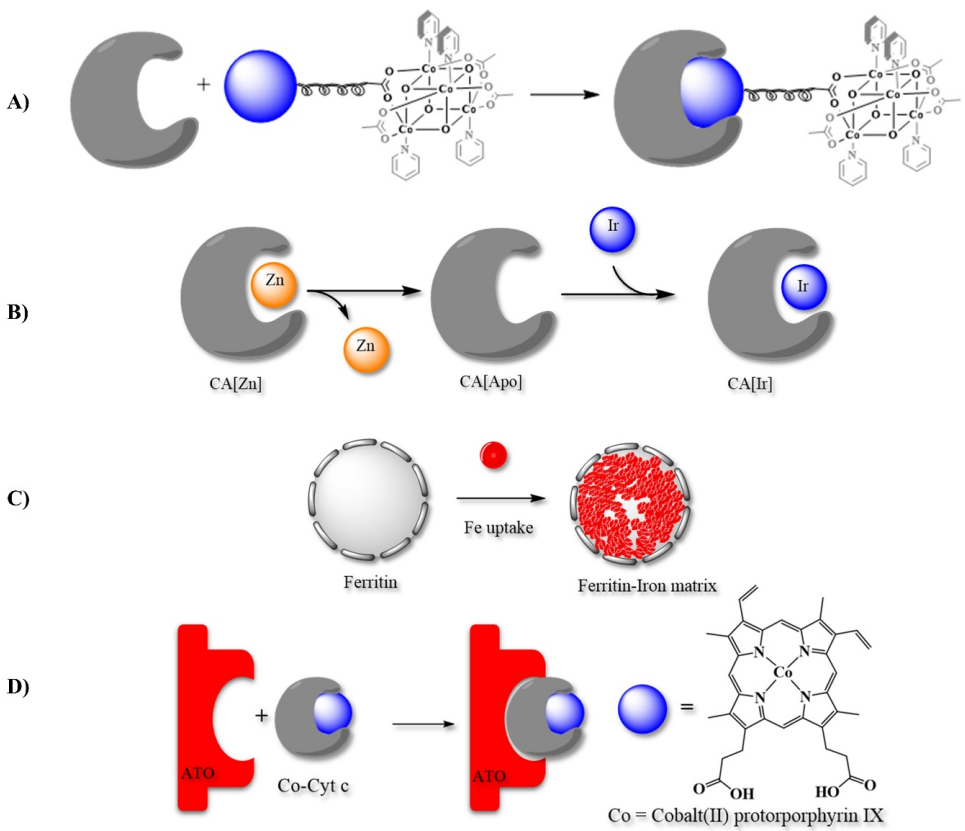

Figure 1.12. Reported artificial metalloenzymes for O_2 evolution based on **(A)** cobalt–cubane conjugation using the biotin-streptavidin technology (adapted from reference 113)[118]; **(B)** Ir^{3+} carbonic anhydrase (adapted from reference 114);[119] **(C)** ferritin (adapted from reference 115);[120] and **(D)** Sb–SnO_2 cobalt–cytochrome C hybrid (adapted from reference 116).[121]

1.6 Aim and outline of this thesis

The aim of this thesis was to develop ArM's capable of catalysing the water oxidation reaction under photocatalytic conditions. Using the dative and supramolecular anchoring strategies, we aimed at modulating the activity of a water oxidation catalyst upon conjugating it to a protein support and hence installing a second coordination sphere around the metal catalyst.

As a first step towards artificial metalloenzymes, **Chapter 2** describes a screening method based on gel electrophoresis and mass spectrometry to study the interaction between a library of ruthenium- and cobalt-based water oxidation catalyst, and the two haem proteins Myoglobin and Cytochrome B5.

Following this screening study, **Chapter 3** describes the development of the first ArM for water oxidation in photocatalytic conditions. Coordination of different stoichiometries of the **CoSalen** complex to the *apo* form of **CB5** (***apo*CB5**) allowed us to show that the ***apo*CB5:CoSalen** ratio determined the catalytic activity of the ArM for water oxidation under blue light irradiation. In addition, the formation of the CoSalen–protein adduct prevented the formation of cobalt nanoparticles, which was observed when the free **CoSalen** complex was used as catalyst in similar conditions.

In **Chapter 4**, using the supramolecular approach we incorporated Ru(bda)– and Ru(tpyda)–like WOCs (bda = 2,2′-bipyridine-6,6′-dicarboxylate; tpyda = [2,2′:6′,2″-terpyridine]-6,6″-dicarboxylate) into Bovine Carbonic Anhydrase (**BCA**) to produce ruthenium-functionalized artificial metalloenzymes. Depending on the arylsulfonamide linkers used for binding the ruthenium complex to the zinc-based catalytic pocket, different ArM were obtained that were either catalytically active or catalytically inactive for photocatalytic water oxidation using a small-molecule $[Ru(bpy)_3]^{2+}$ photosensitizer and peroxodisulfate as sacrificial electron acceptor.

Chapter 5 focused on replacing the small molecule photosensitizer by a new Bovine Serum Albumin-$[Ru(bpy)_3]^{2+}$ conjugate to be used as photosensitizing ArM for photocatalytic water oxidation. By mixing this photon-capturing ArM and the most catalytically active **BCA-Ru$_{WOC}$** ArM developed in Chapter 4, a minimal biomimic system of **PSII** was obtained, in which protein–protein interaction occurred between the **BSA-Ru$_{PS}$** sensitizer and the **BCA–Ru$_{WOC}$** water oxidation

catalyst, to result in photocatalytic water oxidation at low concentrations. The photoproduction of O_2 occurred due to the proximity of the two ArM's.

Finally, **Chapter 6** presents a summary of the thesis, a general discussion, and an outlook on the development of artificial metalloenzymes for artificial photosynthesis.

1.7 References

(1) Nicol, L.; Nawrocki, W. J.; Croce, R. Disentangling the Sites of Non-Photochemical Quenching in Vascular Plants. *Nat. Plants* **2019**, *5* (11), 1177–1183. https://doi.org/10.1038/s41477-019-0526-5.

(2) Croce, R. Light Harvesting in Oxygenic Photosynthesis. *Biochim. Biophys. Acta BBA - Bioenerg.* **2020**, *1861* (4), 148172. https://doi.org/10.1016/j.bbabio.2020.148172.

(3) Whang, D. R.; Apaydin, D. H. Artificial Photosynthesis: Learning from Nature. *ChemPhotoChem* **2018**, *2* (3), 148–160. https://doi.org/10.1002/cptc.201700163.

(4) Wang, Z.; Hu, Y.; Zhang, S.; Sun, Y. Artificial Photosynthesis Systems for Solar Energy Conversion and Storage: Platforms and Their Realities. *Chem. Soc. Rev.* **2022**, *51* (15), 6704–6737. https://doi.org/10.1039/D1CS01008E.

(5) Fang, X.; Kalathil, S.; Reisner, E. Semi-Biological Approaches to Solar-to-Chemical Conversion. *Chem. Soc. Rev.* **2020**, *49* (14), 4926–4952. https://doi.org/10.1039/C9CS00496C.

(6) Keijer, T.; Bouwens, T.; Hessels, J.; Reek, J. N. H. Supramolecular Strategies in Artificial Photosynthesis. *Chem. Sci.* **2021**, *12* (1), 50–70. https://doi.org/10.1039/D0SC03715J.

(7) Qi, J.; Zhang, W.; Cao, R. Solar-to-Hydrogen Energy Conversion Based on Water Splitting. *Adv. Energy Mater.* **2018**, *8* (5), 1701620. https://doi.org/10.1002/aenm.201701620.

(8) Klein, D. M.; Rodríguez-Jiménez, S.; Hoefnagel, M. E.; Pannwitz, A.; Prabhakaran, A.; Siegler, M. A.; Keyes, T. E.; Reisner, E.; Brouwer, A. M.; Bonnet, S. Shorter Alkyl Chains Enhance Molecular Diffusion and Electron Transfer Kinetics between Photosensitisers and Catalysts in CO_2 -Reducing Photocatalytic Liposomes. *Chem. – Eur. J.* **2021**, *27* (68), 17203–17212. https://doi.org/10.1002/chem.202102989.

(9) Pannwitz, A.; Klein, D. M.; Rodríguez-Jiménez, S.; Casadevall, C.; Song, H.; Reisner, E.; Hammarström, L.; Bonnet, S. Roadmap towards Solar Fuel Synthesis at the Water Interface of Liposome Membranes. *Chem. Soc. Rev.* **2021**, *50* (8), 4833–4855. https://doi.org/10.1039/D0CS00737D.

(10) Tao, X.; Zhao, Y.; Wang, S.; Li, C.; Li, R. Recent Advances and Perspectives for Solar-Driven Water Splitting Using Particulate Photocatalysts. *Chem. Soc. Rev.* **2022**, *51* (9), 3561–3608. https://doi.org/10.1039/D1CS01182K.

(11) Liu, C.; van den Bos, D.; den Hartog, B.; van der Meij, D.; Ramakrishnan, A.; Bonnet, S. Ligand Controls the Activity of Light-Driven Water Oxidation Catalyzed by Nickel(II) Porphyrin Complexes in Neutral Homogeneous Aqueous Solutions. *Angew. Chem. Int. Ed.* **2021**, *60* (24), 13463–13469. https://doi.org/10.1002/anie.202103157.

(12) Gao, R.; Zhang, C.; Jun, K.-W.; Kim, S. K.; Park, H.-G.; Zhao, T.; Wang, L.; Wan, H.; Guan, G. Transformation of CO2 into Liquid Fuels and Synthetic Natural Gas Using Green Hydrogen: A Comparative Analysis. *Fuel* **2021**, *291*, 120111. https://doi.org/10.1016/j.fuel.2020.120111.

(13) Mateo, D.; Albero, J.; García, H. Graphene Supported NiO/Ni Nanoparticles as Efficient Photocatalyst for Gas Phase CO2 Reduction with Hydrogen. *Appl. Catal. B Environ.* **2018**, *224*, 563–571. https://doi.org/10.1016/j.apcatb.2017.10.071.

(14) Tahir, M.; Amin, N. A. S. Photo-Induced CO2 Reduction by Hydrogen for Selective CO Evolution in a Dynamic Monolith Photoreactor Loaded with

Ag-Modified TiO2 Nanocatalyst. *Int. J. Hydrog. Energy* **2017**, *42* (23), 15507–15522. https://doi.org/10.1016/j.ijhydene.2017.05.039.

(15) Walter, M. G.; Warren, E. L.; McKone, J. R.; Boettcher, S. W.; Mi, Q.; Santori, E. A.; Lewis, N. S. Solar Water Splitting Cells. *Chem. Rev.* **2010**, *110* (11), 6446–6473. https://doi.org/10.1021/cr1002326.

(16) Yamazaki, H.; Shouji, A.; Kajita, M.; Yagi, M. Electrocatalytic and Photocatalytic Water Oxidation to Dioxygen Based on Metal Complexes. *Coord. Chem. Rev.* **2010**, *254* (21–22), 2483–2491. https://doi.org/10.1016/j.ccr.2010.02.008.

(17) Bofill, R.; García-Antón, J.; Escriche, L.; Sala, X. Chemical, Electrochemical and Photochemical Molecular Water Oxidation Catalysts. *J. Photochem. Photobiol. B* **2015**, *152*, 71–81. https://doi.org/10.1016/j.jphotobiol.2014.10.022.

(18) Sánchez-Murcia, P. A.; Nogueira, J. J.; González, L. Exciton Localization on Ru-Based Photosensitizers Induced by Binding to Lipid Membranes. *J. Phys. Chem. Lett.* **2018**, *9* (4), 683–688. https://doi.org/10.1021/acs.jpclett.7b03357.

(19) Gueret, R.; Poulard, L.; Oshinowo, M.; Chauvin, J.; Dahmane, M.; Dupeyre, G.; Lainé, P. P.; Fortage, J.; Collomb, M.-N. Challenging the $[Ru(Bpy)_3]^{2+}$ Photosensitizer with a Triazatriangulenium Robust Organic Dye for Visible-Light-Driven Hydrogen Production in Water. *ACS Catal.* **2018**, *8* (5), 3792–3802. https://doi.org/10.1021/acscatal.7b04000.

(20) Limburg, B.; Bouwman, E.; Bonnet, S. Rate and Stability of Photocatalytic Water Oxidation Using $[Ru(Bpy)_3]^{2+}$ as Photosensitizer. *ACS Catal.* **2016**, *6* (8), 5273–5284. https://doi.org/10.1021/acscatal.6b00107.

(21) Yersin, H.; Hensler, G.; Gallhuber, E.; Rettig, W. Emission Properties of [Ru(Bpy)3] X2 LnH2O Powders. 3.

(22) Kokhan, O.; Ponomarenko, N. S.; Pokkuluri, P. R.; Schiffer, M.; Mulfort, K. L.; Tiede, David. M. Bidirectional Photoinduced Electron Transfer in

Ruthenium(II)-Tris-Bipyridyl-Modified PpcA, a Multi-Heme *c* -Type Cytochrome from *Geobacter Sulfurreducens*. *J. Phys. Chem. B* **2015**, *119* (24), 7612–7624. https://doi.org/10.1021/jp511558f.

(23) Kärkäs, M. D.; Verho, O.; Johnston, E. V.; Åkermark, B. Artificial Photosynthesis: Molecular Systems for Catalytic Water Oxidation. *Chem. Rev.* **2014**, *114* (24), 11863–12001. https://doi.org/10.1021/cr400572f.

(24) Lewandowska-Andralojc, A.; Polyansky, D. E.; Wang, C.-H.; Wang, W.-H.; Himeda, Y.; Fujita, E. Efficient Water Oxidation with Organometallic Iridium Complexes as Precatalysts. *Phys. Chem. Chem. Phys.* **2014**, *16* (24), 11976. https://doi.org/10.1039/c3cp55101f.

(25) Safdari, R.; Mohammadi, M. R.; Hołyńska, M.; Chernev, P.; Dau, H.; Najafpour, M. M. A Mononuclear Cobalt Complex for Water Oxidation: New Controversies and Puzzles. *Dalton Trans.* **2018**, *47* (46), 16668–16673. https://doi.org/10.1039/C8DT03147A.

(26) Kottrup, K. G.; D'Agostini, S.; van Langevelde, P. H.; Siegler, M. A.; Hetterscheid, D. G. H. Catalytic Activity of an Iron-Based Water Oxidation Catalyst: Substrate Effects of Graphitic Electrodes. *ACS Catal.* **2018**, *8* (2), 1052–1061. https://doi.org/10.1021/acscatal.7b03284.

(27) Nesterov, D.; Nesterova, O. Polynuclear Cobalt Complexes as Catalysts for Light-Driven Water Oxidation: A Review of Recent Advances. *Catalysts* **2018**, *8* (12), 602. https://doi.org/10.3390/catal8120602.

(28) Matheu, R.; Garrido-Barros, P.; Gil-Sepulcre, M.; Ertem, M. Z.; Sala, X.; Gimbert-Suriñach, C.; Llobet, A. The Development of Molecular Water Oxidation Catalysts. *Nat. Rev. Chem.* **2019**, *3* (5), 331–341. https://doi.org/10.1038/s41570-019-0096-0.

(29) Ye, S.; Ding, C.; Liu, M.; Wang, A.; Huang, Q.; Li, C. Water Oxidation Catalysts for Artificial Photosynthesis. *Adv. Mater.* **2019**, *31* (50), 1902069. https://doi.org/10.1002/adma.201902069.

(30) Liu, T.; Zhang, B.; Sun, L. Iron-Based Molecular Water Oxidation Catalysts: Abundant, Cheap, and Promising. *Chem. – Asian J.* **2019**, *14* (1), 31–43. https://doi.org/10.1002/asia.201801253.

(31) You, B.; Sun, Y. Innovative Strategies for Electrocatalytic Water Splitting. *Acc. Chem. Res.* **2018**, *51* (7), 1571–1580. https://doi.org/10.1021/acs.accounts.8b00002.

(32) Qian, R.; Zong, H.; Schneider, J.; Zhou, G.; Zhao, T.; Li, Y.; Yang, J.; Bahnemann, D. W.; Pan, J. H. Charge Carrier Trapping, Recombination and Transfer during TiO2 Photocatalysis: An Overview. *Catal. Today* **2019**, *335*, 78–90. https://doi.org/10.1016/j.cattod.2018.10.053.

(33) Gao, W.; Lu, J.; Zhang, S.; Zhang, X.; Wang, Z.; Qin, W.; Wang, J.; Zhou, W.; Liu, H.; Sang, Y. Suppressing Photoinduced Charge Recombination via the Lorentz Force in a Photocatalytic System. *Adv. Sci.* **2019**, *6* (18), 1901244. https://doi.org/10.1002/advs.201901244.

(34) Zhang, L.; Mohamed, H. H.; Dillert, R.; Bahnemann, D. Kinetics and Mechanisms of Charge Transfer Processes in Photocatalytic Systems: A Review. *J. Photochem. Photobiol. C Photochem. Rev.* **2012**, *13* (4), 263–276. https://doi.org/10.1016/j.jphotochemrev.2012.07.002.

(35) Tian, L.; Li, Z.; Xu, X.; Zhang, C. Advances in Noble Metal (Ru, Rh, and Ir) Doping for Boosting Water Splitting Electrocatalysis. *J. Mater. Chem. A* **2021**, *9* (23), 13459–13470. https://doi.org/10.1039/D1TA01108A.

(36) Kondo, M.; Tatewaki, H.; Masaoka, S. Design of Molecular Water Oxidation Catalysts with Earth-Abundant Metal Ions. *Chem. Soc. Rev.* **2021**, *50* (12), 6790–6831. https://doi.org/10.1039/D0CS01442G.

(37) Kerns, S. A.; Biswas, A.; Minnetian, N. M.; Borovik, A. S. Artificial Metalloproteins: At the Interface between Biology and Chemistry. *JACS Au* **2022**, *2* (6), 1252–1265. https://doi.org/10.1021/jacsau.2c00102.

(38) Schwizer, F.; Okamoto, Y.; Heinisch, T.; Gu, Y.; Pellizzoni, M. M.; Lebrun, V.; Reuter, R.; Köhler, V.; Lewis, J. C.; Ward, T. R. Artificial

Metalloenzymes: Reaction Scope and Optimization Strategies. *Chem. Rev.* **2018**, *118* (1), 142–231. https://doi.org/10.1021/acs.chemrev.7b00014.

(39) Bos, J.; Roelfes, G. Artificial Metalloenzymes for Enantioselective Catalysis. *Curr. Opin. Chem. Biol.* **2014**, *19*, 135–143. https://doi.org/10.1016/j.cbpa.2014.02.002.

(40) Maity, B.; Taher, M.; Mazumdar, S.; Ueno, T. Artificial Metalloenzymes Based on Protein Assembly. *Coord. Chem. Rev.* **2022**, 214593. https://doi.org/10.1016/j.ccr.2022.214593.

(41) Bloomer, B. J.; Clark, D. S.; Hartwig, J. F. Progress, Challenges, and Opportunities with Artificial Metalloenzymes in Biosynthesis. *Biochemistry* **2022**, acs.biochem.1c00829. https://doi.org/10.1021/acs.biochem.1c00829.

(42) Wittwer, M.; Markel, U.; Schiffels, J.; Okuda, J.; Sauer, D. F.; Schwaneberg, U. Engineering and Emerging Applications of Artificial Metalloenzymes with Whole Cells. *Nat. Catal.* **2021**, *4* (10), 814–827. https://doi.org/10.1038/s41929-021-00673-3.

(43) Jung, S.-M.; Lee, J.; Song, W. J. Design of Artificial Metalloenzymes with Multiple Inorganic Elements: The More the Merrier. *J. Inorg. Biochem.* **2021**, *223*, 111552. https://doi.org/10.1016/j.jinorgbio.2021.111552.

(44) Chordia, S.; Narasimhan, S.; Lucini Paioni, A.; Baldus, M.; Roelfes, G. In Vivo Assembly of Artificial Metalloenzymes and Application in Whole-Cell Biocatalysis**. *Angew. Chem. Int. Ed.* **2021**, *60* (11), 5913–5920. https://doi.org/10.1002/anie.202014771.

(45) Zhang, R. K.; Romney, D. K.; Kan, S. B. J.; Arnold, F. H. Directed Evolution of Artificial Metalloenzymes: Bridging Synthetic Chemistry and Biology. In *Artificial Metalloenzymes and MetalloDNAzymes in Catalysis*; Wiley-VCH Verlag GmbH & Co. KGaA: Weinheim, Germany, 2018; pp 137–170. https://doi.org/10.1002/9783527804085.ch5.

(46) Yu, Y.; Hu, C.; Xia, L.; Wang, J. Artificial Metalloenzyme Design with Unnatural Amino Acids and Non-Native Cofactors. *ACS Catal.* **2018**, *8* (3), 1851–1863. https://doi.org/10.1021/acscatal.7b03754.

(47) Bos, J.; Fusetti, F.; Driessen, A. J. M.; Roelfes, G. Enantioselective Artificial Metalloenzymes by Creation of a Novel Active Site at the Protein Dimer Interface. *Angew. Chem. Int. Ed.* **2012**, *51* (30), 7472–7475. https://doi.org/10.1002/anie.201202070.

(48) Hyster, T. K.; Knörr, L.; Ward, T. R.; Rovis, T. Biotinylated Rh(III) Complexes in Engineered Streptavidin for Accelerated Asymmetric C–H Activation. *Science* **2012**, *338* (6106), 500–503. https://doi.org/10.1126/science.1226132.

(49) Allard, M.; Dupont, C.; Muñoz Robles, V.; Doucet, N.; Lledós, A.; Maréchal, J.-D.; Urvoas, A.; Mahy, J.-P.; Ricoux, R. Incorporation of Manganese Complexes into Xylanase: New Artificial Metalloenzymes for Enantioselective Epoxidation. *ChemBioChem* **2012**, *13* (2), 240–251. https://doi.org/10.1002/cbic.201100659.

(50) Boersma, A. J.; Feringa, B. L.; Roelfes, G. Enantioselective Friedel–Crafts Reactions in Water Using a DNA-Based Catalyst. *Angew. Chem.* **2009**, *121* (18), 3396–3398. https://doi.org/10.1002/ange.200900371.

(51) Key, H. M.; Dydio, P.; Clark, D. S.; Hartwig, J. F. Abiological Catalysis by Artificial Haem Proteins Containing Noble Metals in Place of Iron. *Nature* **2016**, *534* (7608), 534–537. https://doi.org/10.1038/nature17968.

(52) Philippart, F.; Arlt, M.; Gotzen, S.; Tenne, S.-J.; Bocola, M.; Chen, H.-H.; Zhu, L.; Schwaneberg, U.; Okuda, J. A Hybrid Ring-Opening Metathesis Polymerization Catalyst Based on an Engineered Variant of the β-Barrel Protein FhuA. *Chem. – Eur. J.* **2013**, *19* (41), 13865–13871. https://doi.org/10.1002/chem.201301515.

(53) Doble, M. V.; Obrecht, L.; Joosten, H.-J.; Lee, M.; Rozeboom, H. J.; Branigan, E.; Naismith, James. H.; Janssen, D. B.; Jarvis, A. G.; Kamer, P.

C. J. Engineering Thermostability in Artificial Metalloenzymes to Increase Catalytic Activity. *ACS Catal.* **2021**, *11* (6), 3620–3627. https://doi.org/10.1021/acscatal.0c05413.

(54) Hirota, S.; Lin, Y.-W. Design of Artificial Metalloproteins/Metalloenzymes by Tuning Noncovalent Interactions. *JBIC J. Biol. Inorg. Chem.* **2018**, *23* (1), 7–25. https://doi.org/10.1007/s00775-017-1506-8.

(55) Sommer, D. J.; Vaughn, M. D.; Ghirlanda, G. Protein Secondary-Shell Interactions Enhance the Photoinduced Hydrogen Production of Cobalt Protoporphyrin IX. *Chem Commun* **2014**, *50* (100), 15852–15855. https://doi.org/10.1039/C4CC06700B.

(56) Song, W. J.; Yu, J.; Tezcan, F. A. Importance of Scaffold Flexibility/Rigidity in the Design and Directed Evolution of Artificial Metallo-β-Lactamases. *J. Am. Chem. Soc.* **2017**, *139* (46), 16772–16779. https://doi.org/10.1021/jacs.7b08981.

(57) Firpo, V.; Le, J. M.; Pavone, V.; Lombardi, A.; Bren, K. L. Hydrogen Evolution from Water Catalyzed by Cobalt-Mimochrome VI*a, a Synthetic Mini-Protein. *Chem. Sci.* **2018**, *9* (45), 8582–8589. https://doi.org/10.1039/C8SC01948G.

(58) Ishida, H.; Maruyama, Y.; Kyakuno, M.; Kodera, Y.; Maeda, T.; Oishi, S. Artificial Metalloproteins with a Ruthenium Tris(Bipyridyl) Complex as the Core. *ChemBioChem* **2006**, *7* (10), 1567–1570. https://doi.org/10.1002/cbic.200600162.

(59) Marchi-Delapierre, C.; Rondot, L.; Cavazza, C.; Ménage, S. Oxidation Catalysis by Rationally Designed Artificial Metalloenzymes. *Isr. J. Chem.* **2015**, *55* (1), 61–75. https://doi.org/10.1002/ijch.201400110.

(60) Oohora, K.; Kihira, Y.; Mizohata, E.; Inoue, T.; Hayashi, T. C(Sp^3)–H Bond Hydroxylation Catalyzed by Myoglobin Reconstituted with Manganese Porphycene. *J. Am. Chem. Soc.* **2013**, *135* (46), 17282–17285. https://doi.org/10.1021/ja409404k.

(61) Okrasa, K.; Kazlauskas, R. J. Manganese-Substituted Carbonic Anhydrase as a New Peroxidase. *Chem. - Eur. J.* **2006**, *12* (6), 1587–1596. https://doi.org/10.1002/chem.200501413.

(62) Peterson, J. R.; Smith, T. A.; Thordarson, P. Photoinduced Reduction of Catalytically and Biologically Active Ru(II)Bisterpyridine–Cytochrome c Bioconjugates. *Chem Commun* **2007**, No. 19, 1899–1901. https://doi.org/10.1039/B702996A.

(63) Monnard, F. W.; Nogueira, E. S.; Heinisch, T.; Schirmer, T.; Ward, T. R. Human Carbonic Anhydrase II as Host Protein for the Creation of Artificial Metalloenzymes: The Asymmetric Transfer Hydrogenation of Imines. *Chem. Sci.* **2013**, *4* (8), 3269. https://doi.org/10.1039/c3sc51065d.

(64) Immoos, C. E.; Di Bilio, A. J.; Cohen, M. S.; Van der Veer, W.; Gray, H. B.; Farmer, P. J. Electron-Transfer Chemistry of Ru−Linker−(Heme)-Modified Myoglobin: Rapid Intraprotein Reduction of a Photogenerated Porphyrin Cation Radical. *Inorg. Chem.* **2004**, *43* (12), 3593–3596. https://doi.org/10.1021/ic049741h.

(65) Serrano-Plana, J.; Rumo, C.; Rebelein, J. G.; Peterson, R. L.; Barnet, M.; Ward, T. R. Enantioselective Hydroxylation of Benzylic C(Sp^3)–H Bonds by an Artificial Iron Hydroxylase Based on the Biotin–Streptavidin Technology. *J. Am. Chem. Soc.* **2020**, *142* (24), 10617–10623. https://doi.org/10.1021/jacs.0c02788.

(66) Roy, A.; Vaughn, M. D.; Tomlin, J.; Booher, G. J.; Kodis, G.; Simmons, C. R.; Allen, J. P.; Ghirlanda, G. Enhanced Photocatalytic Hydrogen Production by Hybrid Streptavidin-Diiron Catalysts. *Chem. – Eur. J.* **2020**, *26* (28), 6240–6246. https://doi.org/10.1002/chem.202000204.

(67) Nastri, F.; D'Alonzo, D.; Leone, L.; Zambrano, G.; Pavone, V.; Lombardi, A. Engineering Metalloprotein Functions in Designed and Native Scaffolds. *Trends Biochem. Sci.* **2019**, *44* (12), 1022–1040. https://doi.org/10.1016/j.tibs.2019.06.006.

(68) Lindskog, S. Structure and Mechanism of Carbonic Anhydrase. *Pharmacol. Ther.* **1997**, *74* (1), 1–20. https://doi.org/10.1016/S0163-7258(96)00198-2.

(69) Krishnamurthy, V. M.; Kaufman, G. K.; Urbach, A. R.; Gitlin, I.; Gudiksen, K. L.; Weibel, D. B.; Whitesides, G. M. Carbonic Anhydrase as a Model for Biophysical and Physical-Organic Studies of Proteins and Protein−Ligand Binding. *Chem. Rev.* **2008**, *108* (3), 946–1051. https://doi.org/10.1021/cr050262p.

(70) Cox, J. D.; Hunt, J. A.; Compher, K. M.; Fierke, C. A.; Christianson, D. W. Structural Influence of Hydrophobic Core Residues on Metal Binding and Specificity in Carbonic Anhydrase II ,. *Biochemistry* **2000**, *39* (45), 13687–13694. https://doi.org/10.1021/bi001649j.

(71) Ferraroni, M.; Cornelio, B.; Sapi, J.; Supuran, C. T.; Scozzafava, A. Sulfonamide Carbonic Anhydrase Inhibitors: Zinc Coordination and Tail Effects Influence Inhibitory Efficacy and Selectivity for Different Isoforms. *Inorganica Chim. Acta* **2018**, *470*, 128–132. https://doi.org/10.1016/j.ica.2017.03.038.

(72) Heinisch, T.; Pellizzoni, M.; Dürrenberger, M.; Tinberg, C. E.; Köhler, V.; Klehr, J.; Häussinger, D.; Baker, D.; Ward, T. R. Improving the Catalytic Performance of an Artificial Metalloenzyme by Computational Design. *J. Am. Chem. Soc.* **2015**, *137* (32), 10414–10419. https://doi.org/10.1021/jacs.5b06622.

(73) Villarejo, A. A Photosystem II-Associated Carbonic Anhydrase Regulates the Efficiency of Photosynthetic Oxygen Evolution. *EMBO J.* **2002**, *21* (8), 1930–1938. https://doi.org/10.1093/emboj/21.8.1930.

(74) Shitov, A. V.; Terentyev, V. V.; Zharmukhamedov, S. K.; Rodionova, M. V.; Karacan, M.; Karacan, N.; Klimov, V. V.; Allakhverdiev, S. I. Is Carbonic Anhydrase Activity of Photosystem II Required for Its Maximum Electron Transport Rate? *Biochim. Biophys. Acta BBA - Bioenerg.* **2018**, *1859* (4), 292–299. https://doi.org/10.1016/j.bbabio.2018.01.009.

(75) Iikuni, S.; Okada, Y.; Shimizu, Y.; Watanabe, H.; Ono, M. Modulation of the Pharmacokinetics of a Radioligand Targeting Carbonic Anhydrase-IX with Albumin-Binding Moieties. *Mol. Pharm.* **2021**, *18* (3), 966–975. https://doi.org/10.1021/acs.molpharmaceut.0c00953.

(76) Takashima, H.; Fukuda, M.; Nakagaki, F.; Ogata, T.; Tsukahara, K. Photoinduced Electron-Transfer Reactions of Carbonic Anhydrase Inhibitor Containing Tris(2,2′-Bipyridine)Ruthenium(II) Analogue. *J. Phys. Chem. B* **2013**, *117* (9), 2625–2635. https://doi.org/10.1021/jp310604w.

(77) Maeshima, K.; Yoshimoto, M. Preparation and Characterization of Carbonic Anhydrase-Conjugated Liposomes for Catalytic Synthesis of Calcium Carbonate Particles. *Enzyme Microb. Technol.* **2017**, *105*, 9–17. https://doi.org/10.1016/j.enzmictec.2017.06.002.

(78) Fu, Y.; Jiang, Y.-B.; Dunphy, D.; Xiong, H.; Coker, E.; Chou, S. S.; Zhang, H.; Vanegas, J. M.; Croissant, J. G.; Cecchi, J. L.; Rempe, S. B.; Brinker, C. J. Ultra-Thin Enzymatic Liquid Membrane for CO2 Separation and Capture. *Nat. Commun.* **2018**, *9* (1), 990. https://doi.org/10.1038/s41467-018-03285-x.

(79) Liu, J.; Chakraborty, S.; Hosseinzadeh, P.; Yu, Y.; Tian, S.; Petrik, I.; Bhagi, A.; Lu, Y. Metalloproteins Containing Cytochrome, Iron–Sulfur, or Copper Redox Centers. *Chem. Rev.* **2014**, *114* (8), 4366–4469. https://doi.org/10.1021/cr400479b.

(80) Yamada, M.; Tamada, T.; Takeda, K.; Matsumoto, F.; Ohno, H.; Kosugi, M.; Takaba, K.; Shoyama, Y.; Kimura, S.; Kuroki, R.; Miki, K. Elucidations of the Catalytic Cycle of NADH-Cytochrome B5 Reductase by X-Ray Crystallography: New Insights into Regulation of Efficient Electron Transfer. *J. Mol. Biol.* **2013**, *425* (22), 4295–4306. https://doi.org/10.1016/j.jmb.2013.06.010.

(81) Rodríguez-Marañón, M. J.; Qiu, F.; Stark, R. E.; White, S. P.; Zhang, X.; Foundling, S. I.; Rodríguez, V.; Schilling, C. L.; Bunce, R. A.; Rivera, M. [13]

C NMR Spectroscopic and X-Ray Crystallographic Study of the Role Played by Mitochondrial Cytochrome b_5 Heme Propionates in the Electrostatic Binding to Cytochrome c. *Biochemistry* **1996**, *35* (50), 16378–16390. https://doi.org/10.1021/bi961895o.

(82) Durley, R. C. E.; Mathews, F. S. Refinement and Structural Analysis of Bovine Cytochrome B5 at 1.5 Å Resolution. *Acta Crystallogr. D Biol. Crystallogr.* **1996**, *52* (1), 65–76. https://doi.org/10.1107/S0907444995007827.

(83) Scott, J. R.; Willie, A.; McLean, M.; Stayton, P. S.; Sligar, S. G.; Durham, B.; Millett, F. Intramolecular Electron Transfer in Cytochrome B5 Labeled with Ruthenium(II) Polypyridine Complexes: Rate Measurements in the Marcus Inverted Region. *J. Am. Chem. Soc.* **1993**, *115* (15), 6820–6824. https://doi.org/10.1021/ja00068a045.

(84) Willie, A.; McLean, M.; Liu, R. Q.; Hilgen-Willis, S.; Saunders, A. J.; Pielak, G. J.; Sligar, S. G.; Durham, B.; Millett, F. Intracomplex Electron Transfer between Ruthenium-65-Cytochrome B5 and Position-82 Variants of Yeast Iso-1-Cytochrome c. *Biochemistry* **1993**, *32* (29), 7519–7525. https://doi.org/10.1021/bi00080a025.

(85) Opdam, L. V.; Polanco, E. A.; de Regt, B.; Lambertina, N.; Bakker, C.; Bonnet, S.; Pandit, A. A Screening Method for Binding Synthetic Metallo-Complexes to Haem Proteins. *Anal. Biochem.* **2022**, *653*, 114788. https://doi.org/10.1016/j.ab.2022.114788.

(86) Phillips, G. N.; Arduini, R. M.; Springer, B. A.; Sligar, S. G. Crystal Structure of Myoglobin Form a Synthetic Gene. *Proteins Struct. Funct. Genet.* **1990**, *7* (4), 358–365. https://doi.org/10.1002/prot.340070407.

(87) Winter, M. B.; McLaurin, E. J.; Reece, S. Y.; Olea, C.; Nocera, D. G.; Marletta, M. A. Ru-Porphyrin Protein Scaffolds for Sensing O_2. *J. Am. Chem. Soc.* **2010**, *132* (16), 5582–5583. https://doi.org/10.1021/ja101527r.

(88) Sreenilayam, G.; Moore, E. J.; Steck, V.; Fasan, R. Metal Substitution Modulates the Reactivity and Extends the Reaction Scope of Myoglobin Carbene Transfer Catalysts. *Adv. Synth. Catal.* **2017**, *359* (12), 2076–2089. https://doi.org/10.1002/adsc.201700202.

(89) Ohashi, M.; Koshiyama, T.; Ueno, T.; Yanase, M.; Fujii, H.; Watanabe, Y. Preparation of Artificial Metalloenzymes by Insertion of Chromium(III) Schiff Base Complexes into Apomyoglobin Mutants. *Angew. Chem. Int. Ed.* **2003**, *42* (9), 1005–1008. https://doi.org/10.1002/anie.200390256.

(90) Ozaki, S.; Matsui, T.; Roach, M. P.; Watanabe, Y. Rational Molecular Design of a Catalytic Site: Engineering of Catalytic Functions to the Myoglobin Active Site Framework. *Coord. Chem. Rev.* **2000**, *198* (1), 39–59. https://doi.org/10.1016/S0010-8545(00)00234-4.

(91) Hamachi, I.; Shinkai, S. Chemical Modification of the Structures and Functions of Proteins by the Cofactor Reconstitution Method. *Eur. J. Org. Chem.* **1999**, *1999* (3), 539–549. https://doi.org/10.1002/(SICI)1099-0690(199903)1999:3<539::AID-EJOC539>3.0.CO;2-F.

(92) Bhosale, S. V.; Kalyankar, M. B.; Bhosale, S. V.; Patil, S. G.; Lalander, C. H.; Langford, S. J.; Nalage, S. V. Supramolecular Self-Assembly of Protoporphyrin IX Amphiphiles into Worm-like and Particular Aggregates. *Supramol. Chem.* **2011**, *23* (3–4), 263–268. https://doi.org/10.1080/10610278.2010.523115.

(93) Hamachi, I.; Tanaka, S.; Shinkai, S. Light-Driven Activation of Reconstituted Myoglobin with a Ruthenium Tris(2,2'-Bipyridine) Pendant. *J. Am. Chem. Soc.* **1993**, *115* (22), 10458–10459. https://doi.org/10.1021/ja00075a111.

(94) Aguilera-Garrido, A.; del Castillo-Santaella, T.; Yang, Y.; Galisteo-González, F.; Gálvez-Ruiz, M. J.; Molina-Bolívar, J. A.; Holgado-Terriza, J. A.; Cabrerizo-Vílchez, M. Á.; Maldonado-Valderrama, J. Applications of Serum Albumins in Delivery Systems: Differences in Interfacial Behaviour

and Interacting Abilities with Polysaccharides. *Adv. Colloid Interface Sci.* **2021**, *290*, 102365. https://doi.org/10.1016/j.cis.2021.102365.

(95) Feng, L.; Fang, J.; Zeng, X.; Liu, H.; Zhang, J.; Huang, L.; Guo, Z.; Zhuang, R.; Zhang, X. 68Ga-Labeled Maleimide for Blood Pool and Lymph PET Imaging through Covalent Bonding to Serum Albumin In Vivo. *ACS Omega* **2022**, *7* (32), 28597–28604. https://doi.org/10.1021/acsomega.2c03505.

(96) Kandagal, P. B.; Ashoka, S.; Seetharamappa, J.; Shaikh, S. M. T.; Jadegoud, Y.; Ijare, O. B. Study of the Interaction of an Anticancer Drug with Human and Bovine Serum Albumin: Spectroscopic Approach. *J. Pharm. Biomed. Anal.* **2006**, *41* (2), 393–399. https://doi.org/10.1016/j.jpba.2005.11.037.

(97) Mondal, P.; Bose, A. Spectroscopic Overview of Quercetin and Its Cu(II) Complex Interaction with Serum Albumins. *BioImpacts* **2019**, *9* (2), 115–121. https://doi.org/10.15171/bi.2019.15.

(98) Jattinagoudar, L.; Meti, M.; Nandibewoor, S.; Chimatadar, S. Evaluation of the Binding Interaction between Bovine Serum Albumin and Dimethyl Fumarate, an Anti-Inflammatory Drug by Multispectroscopic Methods. *Spectrochim. Acta. A. Mol. Biomol. Spectrosc.* **2016**, *156*, 164–171. https://doi.org/10.1016/j.saa.2015.11.026.

(99) Bagoji, A. M.; Buddanavar, A. T.; Gokavi, N. M.; Nandibewoor, S. T. Characterization of the Binding and Conformational Changes of Bovine Serum Albumin upon Interaction with Antihypertensive Olmesartan Medoxomil. *J. Mol. Struct.* **2019**, *1179*, 269–277. https://doi.org/10.1016/j.molstruc.2018.10.089.

(100) Wang, Q.; Huang, C.; Jiang, M.; Zhu, Y.; Wang, J.; Chen, J.; Shi, J. Binding Interaction of Atorvastatin with Bovine Serum Albumin: Spectroscopic Methods and Molecular Docking. *Spectrochim. Acta. A. Mol. Biomol. Spectrosc.* **2016**, *156*, 155–163. https://doi.org/10.1016/j.saa.2015.12.003.

(101) Karami, E.; Behdani, M.; Kazemi-Lomedasht, F. Albumin Nanoparticles as Nanocarriers for Drug Delivery: Focusing on Antibody and Nanobody

Delivery and Albumin-Based Drugs. *J. Drug Deliv. Sci. Technol.* **2020**, *55*, 101471. https://doi.org/10.1016/j.jddst.2019.101471.

(102) Solanki, R.; Rostamabadi, H.; Patel, S.; Jafari, S. M. Anticancer Nano-Delivery Systems Based on Bovine Serum Albumin Nanoparticles: A Critical Review. *Int. J. Biol. Macromol.* **2021**, *193*, 528–540. https://doi.org/10.1016/j.ijbiomac.2021.10.040.

(103) Zhang, Y.-Z.; Zhou, B.; Liu, Y.-X.; Zhou, C.-X.; Ding, X.-L.; Liu, Y. Fluorescence Study on the Interaction of Bovine Serum Albumin with P-Aminoazobenzene. *J. Fluoresc.* **2008**, *18* (1), 109–118. https://doi.org/10.1007/s10895-007-0247-4.

(104) Wang, C.; O'Hagan, M. P.; Willner, B.; Willner, I. Bioinspired Artificial Photosynthetic Systems. *Chem. – Eur. J.* **2022**, *28* (9). https://doi.org/10.1002/chem.202103595.

(105) Meng, S.-L.; Li, X.-B.; Tung, C.-H.; Wu, L.-Z. Nitrogenase Inspired Artificial Photosynthetic Nitrogen Fixation. *Chem* **2021**, *7* (6), 1431–1450. https://doi.org/10.1016/j.chempr.2020.11.002.

(106) Cerón, M. R.; Izquierdo, M.; Alegret, N.; Valdez, J. A.; Rodríguez-Fortea, A.; Olmstead, M. M.; Balch, A. L.; Poblet, J. M.; Echegoyen, L. A Photoactive Semisynthetic-Metalloenzyme-Exhibits-Complete-Selectivity for Co2 Reduction in Water. *Chem. Commun.* **2016**, *52* (1), 64–67. https://doi.org/10.1039/C5CC07416A.

(107) Hosseinzadeh, P.; Lu, Y. Design and Fine-Tuning Redox Potentials of Metalloproteins Involved in Electron Transfer in Bioenergetics. *Biochim. Biophys. Acta BBA - Bioenerg.* **2016**, *1857* (5), 557–581. https://doi.org/10.1016/j.bbabio.2015.08.006.

(108) Metalloenzyme-Inspired Systems for Alternative Energy Harvest.Pdf.

(109) Orio, M.; Pantazis, D. A. Successes, Challenges, and Opportunities for Quantum Chemistry in Understanding Metalloenzymes for Solar Fuels

Research. *Chem. Commun.* **2021**, *57* (33), 3952–3974. https://doi.org/10.1039/D1CC00705J.

(110) Bachmeier, A.; Murphy, B. J.; Armstrong, F. A. A Multi-Heme Flavoenzyme as a Solar Conversion Catalyst. *J. Am. Chem. Soc.* **2014**, *136* (37), 12876–12879. https://doi.org/10.1021/ja507733j.

(111) Rapson, T. D.; Ju, H.; Marshall, P.; Devilla, R.; Jackson, C. J.; Giddey, S.; Sutherland, T. D. Engineering a Solid-State Metalloprotein Hydrogen Evolution Catalyst. *Sci. Rep.* **2020**, *10* (1), 3774. https://doi.org/10.1038/s41598-020-60730-y.

(112) Esmieu, C.; Raleiras, P.; Berggren, G. From Protein Engineering to Artificial Enzymes – Biological and Biomimetic Approaches towards Sustainable Hydrogen Production. *Sustain. Energy Fuels* **2018**, *2* (4), 724–750. https://doi.org/10.1039/C7SE00582B.

(113) Silver, S. C.; Niklas, J.; Du, P.; Poluektov, O. G.; Tiede, D. M.; Utschig, L. M. Protein Delivery of a Ni Catalyst to Photosystem I for Light-Driven Hydrogen Production. *J. Am. Chem. Soc.* **2013**, *135* (36), 13246–13249. https://doi.org/10.1021/ja405277g.

(114) Call, A.; Casadevall, C.; Romero-Rivera, A.; Martin-Diaconescu, V.; Sommer, D. J.; Osuna, S.; Ghirlanda, G.; Lloret-Fillol, J. Improved Electro- and Photocatalytic Water Reduction by Confined Cobalt Catalysts in Streptavidin. *ACS Catal.* **2019**, *9* (7), 5837–5846. https://doi.org/10.1021/acscatal.8b04981.

(115) Soltau, S. R.; Dahlberg, P. D.; Niklas, J.; Poluektov, O. G.; Mulfort, K. L.; Utschig, L. M. Ru–Protein–Co Biohybrids Designed for Solar Hydrogen Production: Understanding Electron Transfer Pathways Related to Photocatalytic Function. *Chem. Sci.* **2016**, *7* (12), 7068–7078. https://doi.org/10.1039/C6SC03121H.

(116) Zhang, J. Z.; Reisner, E. Advancing Photosystem II Photoelectrochemistry for Semi-Artificial Photosynthesis. *Nat. Rev. Chem.* **2020**, *4* (1), 6–21. https://doi.org/10.1038/s41570-019-0149-4.

(117) Sokol, K. P.; Robinson, W. E.; Warnan, J.; Kornienko, N.; Nowaczyk, M. M.; Ruff, A.; Zhang, J. Z.; Reisner, E. Bias-Free Photoelectrochemical Water Splitting with Photosystem II on a Dye-Sensitized Photoanode Wired to Hydrogenase. *Nat. Energy* **2018**, *3* (11), 944–951. https://doi.org/10.1038/s41560-018-0232-y.

(118) Olshansky, L.; Huerta-Lavorie, R.; Nguyen, A. I.; Vallapurackal, J.; Furst, A.; Tilley, T. D.; Borovik, A. S. Artificial Metalloproteins Containing Co_4O_4 Cubane Active Sites. *J. Am. Chem. Soc.* **2018**, *140* (8), 2739–2742. https://doi.org/10.1021/jacs.7b13052.

(119) Kim, M.-C.; Lee, S.-Y. Catalytic Water Oxidation by Iridium-Modified Carbonic Anhydrase. *Chem. - Asian J.* **2018**, *13* (3), 334–341. https://doi.org/10.1002/asia.201701543.

(120) Abdi, Z.; Bagheri, R.; Song, Z.; Najafpour, M. M. Water Oxidation by Ferritin: A Semi-Natural Electrode. *Sci. Rep.* **2019**, *9* (1), 11499. https://doi.org/10.1038/s41598-019-47661-z.

(121) Casadevall, C.; Zhang, H.; Chen, S.; Sommer, D. J.; Seo, D.-K.; Ghirlanda, G. Photoelectrochemical Water Oxidation by Cobalt Cytochrome C Integrated-ATO Photoanode. *Catalysts* **2021**, *11* (5), 626. https://doi.org/10.3390/catal11050626.